

Crack Propagation Behavior Based on the Characteristic of the Interaction Between Two Fatigue Cracks

Sam-Hong Song*, Byoung-Ho Choi** and Jun-Soo Bae**

(Received November 26, 1996)

Stress interaction fields, which are caused by propagating cracks and other defects, can weaken structures. In this study, crack behavior in the interaction field caused by two different cracks is experimentally studied. In the experiment, the vertical distance between two cracks and the applied stresses are varied to create different stress interaction fields. In addition, the effect of the plastic zone is used to examine the crack propagation path and rate. Three types of crack propagation in the interaction field were found, and the crack propagating path and rate of two cracks were significantly affected according to different applied stresses as each crack propagates. These results are attributed to the effect of the size and shape of the plastic zone.

Key Words : Crack Interaction, Fatigue Life, Plastic Zone, Crack Propagation Rate, Finite Element Analysis, Crack Propagation Path

1. Introduction

If there are defects or cracks on the inner side or surface of a structure, cracks will propagate and eventually the structure can be fractured. Otherwise, the crack propagation behavior can interact with other defects and cracks, and there have been many studies on this subject. In the case of two holes located closely, the stress interaction effect were studied by the Finite Element Method (Song et. al., 1994), as well as the case of holes arranged in a particular direction (Song et. al., 1995). It was also shown that the plastic zone around the crack tip plays a central role in determining the crack growth speed and direction (Wu et. al., 1994). For the study of the interaction between cracks, stress intensity factors (SIF) were calculated by an integral equation (Rubinstein, 1988) and the SIF of arbitrarily oriented cracks was also calculated in the case of anisotropic materials (Mauge et. al., 1994). According to

these studies, the SIF increases when crack, hole and inclusion with lower stiffness are located ahead of the crack tip and decreases when they are located after the crack tip.

However, not only are the studies on the interaction effect between cracks limited, but most of the studies deal with variations of SIF. There are relatively few studies on the life evaluation or crack propagation behavior in cracked structures when the cracks interact. However, estimation of failure life or crack propagation behavior is important for safety evaluation of a structure. In this study, the vertical distance between two cracks is first varied to generate different stress fields, and the experimental results are compared with elasto-plastic finite element method data to analyze the interaction behavior under different applied stresses.

2. Experimental Procedure

The material used in this study is aluminium alloy, Al-5086, and its chemical composition and mechanical properties are shown in Table 1, 2. Tests were carried out using a bending and tor-

* Dept. of Mechanical Engineering, Korea University

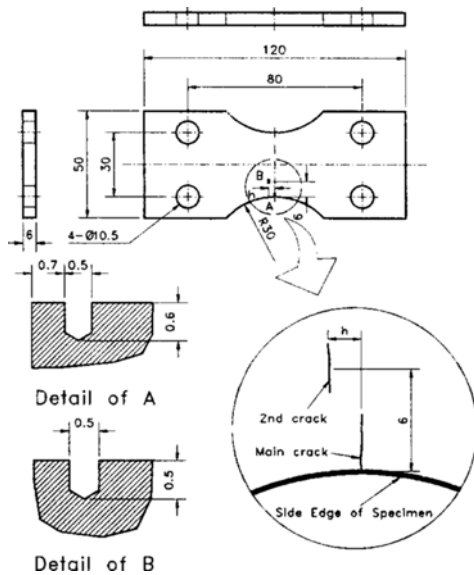
** Graduate School, Korea University

Table 1 Chemical composition of the testing material.

Material	Composition (weight percent, %)			
	Al	Mn	Mg	Cr
Al-5086	95.4	0.4	4.0	0.15

Table 2 Mechanical properties of the testing material.

Yield stress (MPa)	Ultimate stress (MPa)	Elongation (%)	Elasticity modulus (GPa)	Poisson's ratio
190	260	22	62.4	0.32

**Fig. 1** Geometry of specimen.

sion fatigue tester (TB-10, Shimadzu). In the experiment, the cycle ratio (R) was -1 and the waveform was sinusoidal with 33.3 Hz of frequency.

Figure 1 shows the test specimen and geometries of the hole defects to make the cracks. One of the hole defects was machined to make the main crack at 0.7 mm beneath the specimen with 0.5 mm in diameter and 0.6 mm in height. When the length of the main crack reached 2.5 mm, the second hole is machined at 6 mm from the left edge to make the 2nd crack be 0.5 mm in both diameter and height. The vertical distance between the main crack and the 2nd crack (h) was varied at 0, 0.5, 0.7, 1.0, 2.0 mm respectively, with

a maximum stress of cyclic load of 90 MPa. In addition, the experiment was performed with maximum stress varied at 90, 105 MPa in $h=0.5$ mm, and at 90, 120 MPa in $h=1.0$ mm respectively.

In the finite element analysis, the commercial program NISA made by EMRC Co. Ltd. was used. Plasto-elastic FE analysis was performed with 10 models at two stress cases of 90, 120 MPa when $h=0.5$ mm. The number of elements and nodes used in the model are given in Table 3. In FEM, the element used was 2-dimensional 8-node isoparametric and the singularity element was used to evaluate the stress singularity of the crack tip.

3. Test Results and Discussion

3.1 Location of the 2nd crack and crack behavior

3.1.1 Growth of the 2nd crack

There are three types of crack propagation as shown in Fig. 2. The actual cracks start from holes, but if one of the cracks initiates and grows up to a certain length, the effect of a hole will be small relative to the effect of a crack, so it is assumed that there are only cracks. In type A, the main crack and the 2nd crack coalesce, in which case the vertical distance h is small. From Forsyth (1983), the vertical distance is dependent on the plastic zone size (PZS) of two cracks. If the PZS is large, two cracks can be united even though the vertical distance is long. In type B, the main crack

Table 3 Elasto-plastic finite element analysis model.

Applied stress	Model number	No. of nodes	No. of elements
90 MPa	SPEC90-1	2421	764
	SPEC90-2	2339	708
	SPEC90-3	2192	688
	SPEC90-4	2328	728
	SPEC90	2314	730
120 MPa	SPEC120-1	2488	782
	SPEC120-2	2092	658
	SPEC120-3	1966	616
	SPEC120-4	2248	708
	SPEC120	2477	778

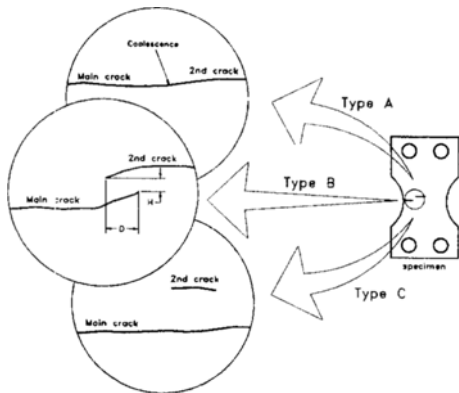


Fig. 2 Configuration of crack propagation type under crack interaction.

and the 2nd crack stop in a curve, which can be seen in the case of $h=0.5, 1.0$ mm. In $h=0.7, 2.0$ mm (Type C), the 2nd crack at first grows but stops immediately while the main crack grows continuously. In the case of $h=0.7$ mm, because the value of h is between 0.5 and 1.0 mm, the type of crack propagation seems to be type B. But as the initiation of the 2nd crack comes late in this experiment, the interaction effect is too small to be type B. If the 2nd crack grows earlier, the type of the propagation will be type B.

3.1.2 a-N' curve of total crack

Figure 3 shows the $a-N'$ curve between crack length and life after the 2nd crack starts to grow. The modified number of cycles N' is represented

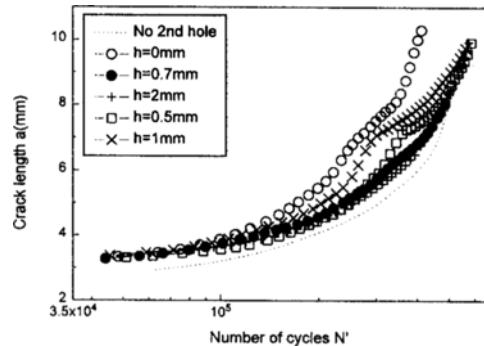


Fig. 3 Relation between crack length and number of cycles.

as,

$$N' = N - N_{2.5} \tag{1}$$

where

N = Number of cycles

$N_{2.5}$ = Number of cycles when the main crack reaches 2.5mm (that is, after machining 2nd hole)

With the growth of the 2nd crack and the crack interaction following it, the shape of the $a-N'$ curve changes at each type. In the case of $h=0$ mm (type A), the life of the specimen at $a=10$ mm is about 26% shorter than that of the case without the 2nd crack at 90 MPa. This result is similar to that reported in work on Multiple-site-damage (MSD) cracks (e. g. Partl et. al., 1993), which studied the life evaluation of three MSD cracks in

Table 4 Number of cycles at $a=10$ mm.

Vertical distance h (mm)	Number of cycles at $a=10$ mm	Rate of variation (%)
Non-2nd crack	5.70×10^5	—
0	4.20×10^5	-26.32
0.5	5.99×10^5	5.44
0.7	6.11×10^5	7.19
1	6.05×10^5	6.14
2	6.01×10^5	5.44

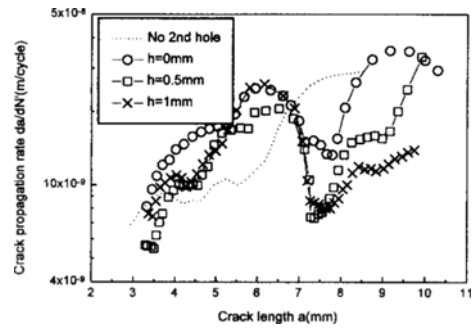
aluminum alloy 2024-T3. They showed that there was a 20% life reduction compared to that of the case with one hole. For the other cases ($h=0.5, 0.7, 1.0, 2.0$ mm), the final life is almost the same as that of the case without the 2nd crack. It can be concluded that the total life is hardly changed in the case of type B and C. Table 4 shows the life at $a=10$ mm just before failure.

Observe that the configuration of $a-N'$ is different in each type. In the case of type B, there are two distinct phenomena: acceleration in closing and deceleration after passing each crack tip. Otherwise, there are vague phenomena of acceleration and deceleration in type C.

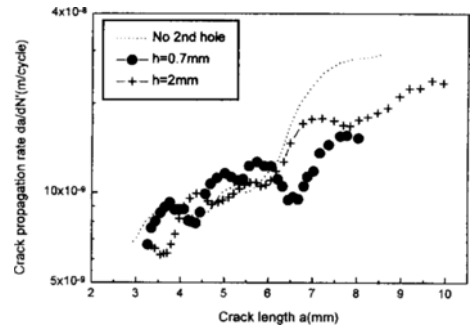
3.1.3 Crack propagation rate of the total crack

Figure 4 shows the crack propagation rate of the total crack.

As seen from Fig. 4, the crack propagation rate increases almost uniformly in the case of no second crack (dashed line). In type A ($h=0$ mm), crack propagation rate increases sharply before coalescence and decreases up to the period of completion of the internal crack growth after coalescence. After that period, the crack propagation rate recovers its original speed. Fig. 4(a) shows that the overall shape of crack propagation rate of type B ($h=0.5, 1.0$ mm) is similar with that of type A. However, in spite of having a similar rising portion as type A, the reduction portion is larger than that of type A, so that there can be a difference in the total life. In this case, that is, according to the two crack tips approaching each other, crack propagation rate increases because of interaction, but after meeting in the x direction of



(a) Type A and B ($h=0, 0.5, 1.0$ mm)



(b) Type C ($h=0.7, 2.0$ mm)

Fig. 4 Relation between crack length and crack propagation rate.

the two crack tips, the total life is governed by the propagation rate of the 2nd crack. It is known that this crack component is slow until now. Figure 4(b) shows da/dN' for $h=0.7, 2.0$ mm. It is seen from this figure that there is little effect of the 2nd crack in $h=2.0$ mm and small variation of crack propagation rate which is not effective relative to the formal two cases. It is due to the fact that life and propagation rate are not affected by small stress interaction such as type C. So if h is up to 2 mm, the effect of the 2nd crack is

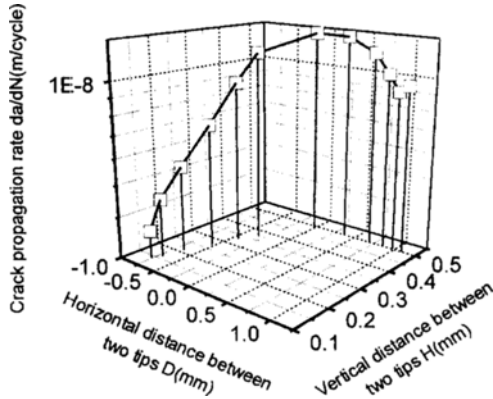


Fig. 5 Relation between crack propagation and relative distance of two tips ($h=0.5$ mm).

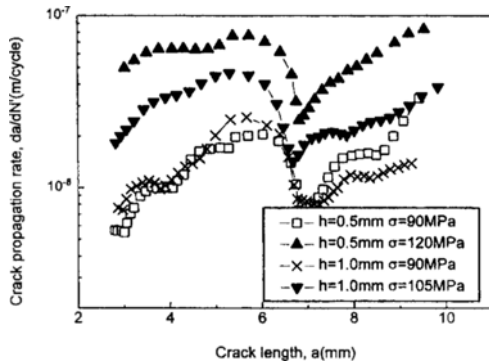


Fig. 6 Relation between crack length and crack propagation rate at different stress.

vanished as shown in crack propagation rate or a -N' diagram. In Figure 5 shows the crack propagation rate of the main crack according to the change of D and H (refer to Fig. 2). It is known that crack propagation rate of the main crack increases as D goes to 0 and decreases as D goes to (-) and H decreases.

3.2 Crack propagation behavior according to the variation of stress

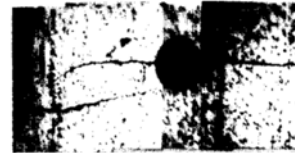
3.2.1 Configuration of crack propagation according to the variation of stress

Figure 6 shows the crack propagation rate for $\sigma_{max}=90$ MPa, 120 MPa in $h=0.5$ mm and $\sigma_{max}=90$ MPa, 105 MPa in $h=1.0$ mm.

It is known that crack propagation rate increases according to the applied stress, but the



(a) $\sigma_{max}=90$ MPa



(b) $\sigma_{max}=120$ MPa

Fig. 7 Shapes of crack propagation at different stress.

configuration of the increase and decrease of propagation rate is shown only as a vertical movement. In this experiment, by changing the applied stress at constant h, all cases have crack propagation of type B. It is shown that crack propagation rate and failure life are affected by change of stress in the propagating crack. Meanwhile, they are shown in Fig. 7 of photographs of crack propagation at $\sigma_{max}=90$ MPa and 120 MPa in $h=0.5$ mm.

It is shown in the photograph that the direction of crack propagation changes earlier at $\sigma_{max}=120$ MPa. The arrow marks in the photograph indicate the start point at which the crack curves. The distance between two arrows at $\sigma_{max}=120$ MPa is larger than that at $\sigma_{max}=90$ MPa. It is thought that because the plastic zone size (PZS) at $\sigma_{max}=120$ MPa is larger than $\sigma_{max}=90$ MPa, cracks can be affected by interaction effect. A finite element analysis is carried out to determine this.

3.2.2 Finite element analysis

To examine changes of PZS when a crack changes its path in propagating, a plasto-elastic finite element analysis is performed. To consider PZS, Von Mises yield stress as follows is used:

$$\begin{aligned} \sigma_y &= \sigma_{eq} \\ &= \frac{1}{\sqrt{2}} \sqrt{(\sigma_1 - \sigma_2)^2 + (\sigma_2 - \sigma_3)^2 + (\sigma_3 - \sigma_1)^2} \end{aligned} \quad (2)$$

There are five models in each stress case (90 and

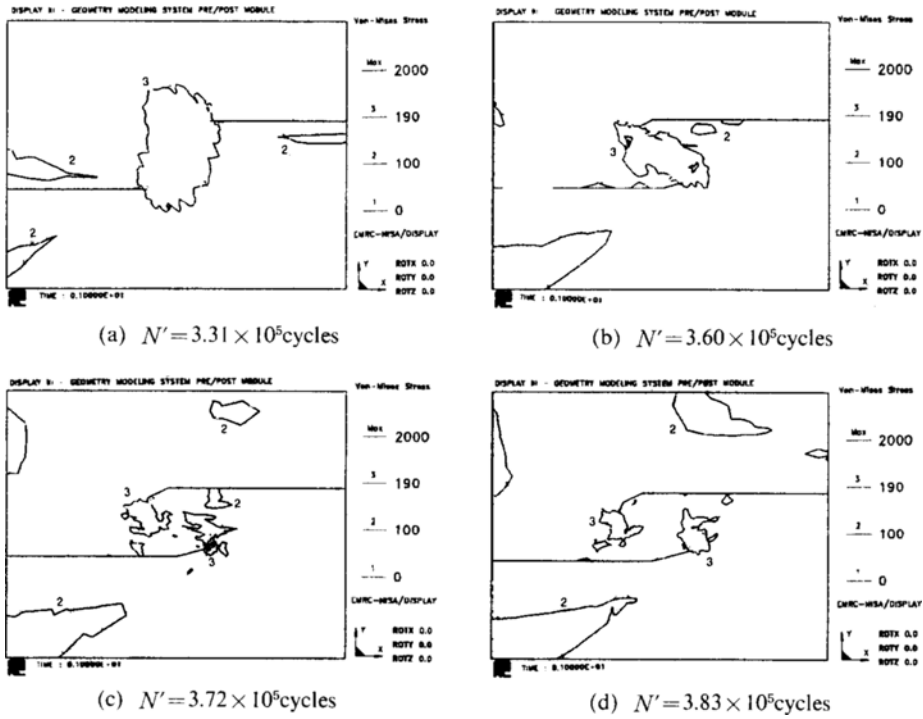


Fig. 8 Equivalent stress distribution at 90 MPa.

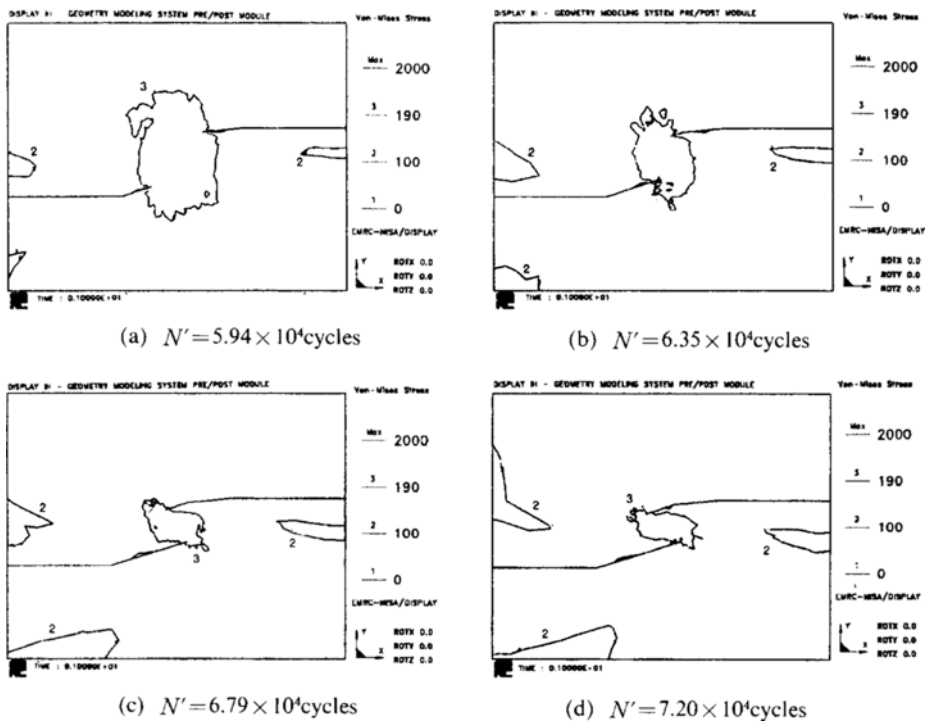


Fig. 9 Equivalent stress distribution at 120 MPa.

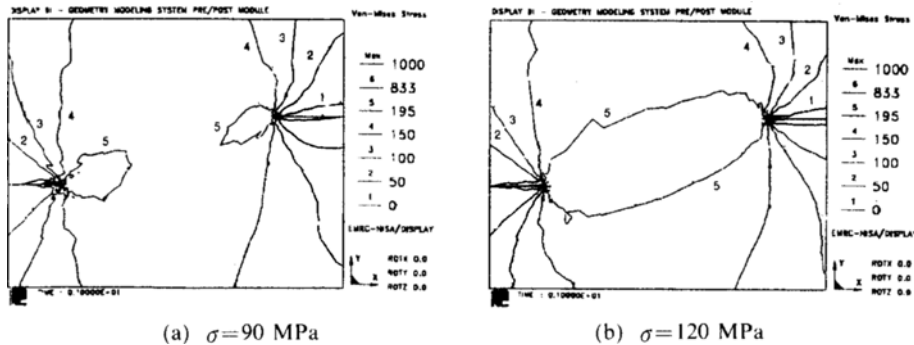


Fig. 10 Stress distribution at different stress (Same D & H).

120 MPa respectively). Actually crack goes curvedly, each model is constructed under the assumption of straight propagating cracks in 0.16 mm at the lowest based on the path observed in the experiment. Figure 8 shows the equivalent stress distribution in the case of $\sigma_{max}=90$ MPa, and in Fig. 9 the case of $\sigma_{max}=120$ MPa.

It is shown in two figures(Fig. 8 and Fig. 9) that the shape and the size of the plastic zone change distinctly before and after $D=0$. So, crack propagation rate and path can be changed by interaction though h is equal. Figure 10 shows the stress distribution in the case of the same D and H ($D=1.5$ mm, $H=0.5$ mm) at different stresses. It can be seen that PZS at $\sigma_{max}=120$ MPa is larger and the interaction effect is more sensitive.

Forsyth(1983) proposed a plastic zone change model(Fig. 11) based on the change of stress intensity factor(K) which affects the change of PZS directly. However, though K increases before $D=0$ (Mauge et. al., 1994), this increase of K cannot explain the increase of PZS . It is due to the fact that the area of producing plastic zone becomes small relatively. They can be seen in Fig. 9 of the FEM results. Accordingly, as there is no consideration of variation of configuration of the area of producing plastic zone by two crack's propagation in Forsyth's model. So it cannot describe the relationship between PZS and crack interaction with this model effectively.

Therefore the relationship between variable configuration and PZS must be considered to estimate the effect of crack interaction. In general, the variation of SIF is related to that of PZS in

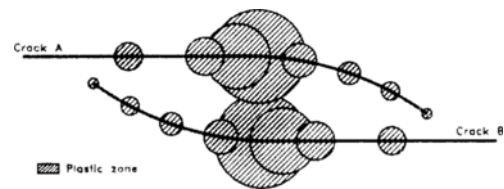


Fig. 11 Crack tip plastic zone size changes for approaching and passing offset cracks by Forsyth.

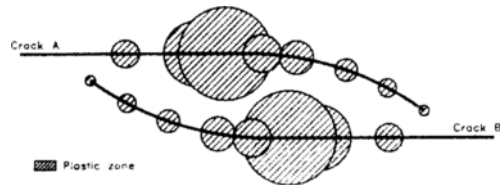


Fig. 12 Modified model of crack tip plastic zone size changes for approaching and passing offset cracks.

the case of unique cracks, so crack propagation rate is represented as follows:

$$\frac{da}{dN} = f(PZS, R) \tag{3}$$

where

R : stress ratio

But variation of configuration must be considered in crack interaction field as follows:

$$\frac{da}{dN} = f(PZS, R, D, H) \tag{4}$$

Figure 12 shows the new model according to Eq. (4). The location of maximum PZS is not where $D=0$ but where is slightly prior to this.

Though PZS becomes small from the location of maximum PZS to that of $D=0$, an actual interaction effect becomes large in opposition to the increase of SIF .

4. Conclusion

In this paper, the crack behavior is studied by experiment in the interacted field generated by two different cracks and is examined to the plastic zone by FEM. The obtained results are as follows:

(1) There are three types of crack propagation, and each type has a different crack propagation rate behavior, e.g., acceleration and deceleration.

(2) In the case of type A, total life is reduced by 26% compared to the case when no second crack exists. But in other cases, total life is scarcely changed in spite of the fact that the change of the configuration of the crack propagation rate is changed in each case.

(3) In type B, the crack propagation rate of the main crack increases before $D=0$, and decreases rapidly after $D=0$. The crack propagation path and rate of the two cracks are significantly changed by different applied stresses as each crack propagates, which can be explained by the plastic zone. But the aspect of variation of plastic zone cannot be explained only by its size and its configuration must be considered together.

References

- Forsyth, P. J. E., 1983, "A Unified Description of Micro and Macroscopic Fatigue Crack Behaviour," *International Journal of Fatigue*, pp. 3~14.
- Mauge, C. and Kachanov, M., 1994, "Anisotropic Material with Interacting Arbitrarily Oriented Cracks. Stress Intensity Factors and Crack-Microcrack Interactions," *International Journal of Fracture*, Vol. 65, pp. 115~139.
- Partl, O. and Schijve, J., 1993, "Multiple-Site Damage in 2024-T3 Alloy Sheet," *International Journal of Fatigue*, Vol. 15 No. 4, pp. 293~299.
- Rubinstein, A. A. and Choi, H. C., 1988, "Macrocrack Interaction with Transverse Array of Microcracks," *International Journal of Fracture*, Vol. 36, pp. 15~26.
- Song, S. H. and Bae, J. S., 1995, "Crack Initiation and Propagation in Stress Interaction Field," *Proceedings of the KSME Spring Annual Meeting '95 (I)*, pp. 196~200.
- Song, S. H. and Kim, J. B., 1994, "Analysis of Stress Distribution Around Micro Hole by F. E. M. -Stress Distribution around Defects and Inclusions-," *Transactions of the KSME*, Vol. 18, No. 3, pp. 555~564.
- Wu, S., Ivanova, E. and Chudnovsky, A., 1994, "The effect of a process zone on the fracture path in a complex stress field," *International Journal of Fracture*, Vol. 67, pp. R13~R19.